Semi-quantitative predictions of hot tearing and cold cracking in aluminum DC casting using numerical process simulator

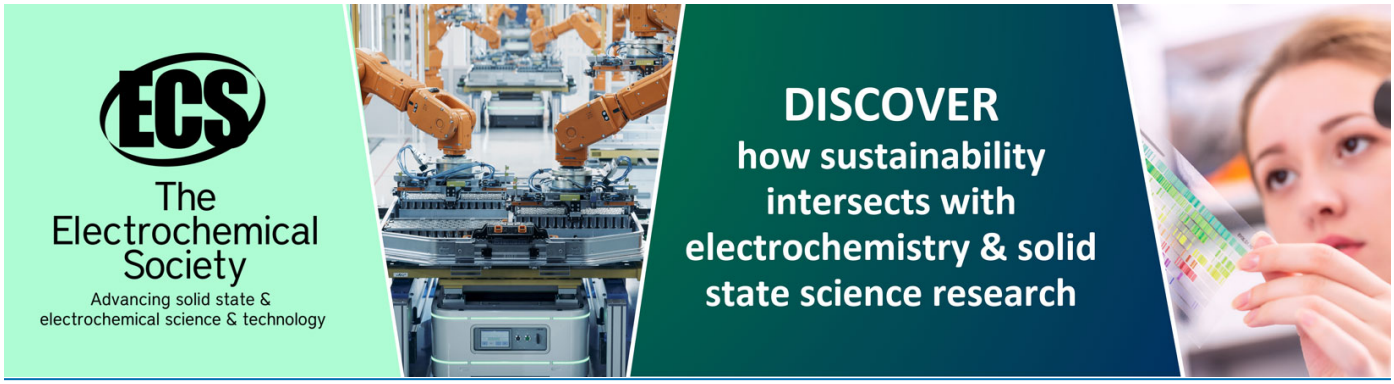

Semi-quantitative predictions of hot tearing and cold cracking in aluminum DC casting using numerical process simulator

T Subroto[1,2], A Miroux[1,2], D Mortensen[3], M M'Hamdi[4], D G Eskin[5] and L Katgerman[2]

[1] Materials innovation institute (M2i), Mekelweg 2, Delft, 2628CD, The Netherlands
[2] Dept. of Material Science and Engineering, Delft University of Technology, Mekelweg 2, Delft, 2628CD, The Netherlands
[3] Institute for Energy Technology, N-2027 Kjeller, Norway
[4] SINTEF Materials and Chemistry, P.B. 124 Blindern, N-0314 Oslo, Norway
[5] BCAST, Brunel University, Uxbridge, Middlesex, UB8 3PH, United Kingdom

E-mail: t.subroto@m2i.nl

Abstract. Cracking is one of the most critical defects that may occur during aluminum direct-chill (DC) casting. There are two types of cracking typical of DC casting: hot tearing and cold cracking. To study and predict such defects, currently we are using a process simulator, ALSIM. ALSIM is able to provide semi-quantitative predictions of hot tearing and cold cracking susceptibility. In this work, we performed benchmark tests using predictions of both types of cracks and experimental results of DC casting trials. The trials series resulted in billets with hot tearing as well as cold cracking. The model was also used to study the influence of several casting variables such as casting speed and inlet geometry with respect to the cracking susceptibility in the ingots. In this work, we found that the sump geometry was changed by the feeding scheme, which played an important role in hot tear occurrence. Moreover, increasing the casting speed also increased the hot tear and cold crack susceptibility. In addition, from the result of simulation, we also observed a phenomenon that supported the hypotheses of connection between hot tearing and cold cracking.

1. Introduction

Direct-chill (DC) casting is a common technique used to produce aluminum billets and ingots owing to its robustness and relative simplicity [1]. However due to the nature of this technique, which introduces a high temperature gradient between the ingot and cooling surface, defects can form during DC casting such as ingot distortion and cracks. The latter is considered one of the worst forms of defects because it is not only capable of reducing ingot quality, but cracks may also occur throughout the entire ingot, thus the ingot has to be fully scrapped [2]. There are two types of cracks that could occur during DC casting; hot tearing when the alloy is still in the semi solid state and cold cracking when the alloy is already in a fully solid. Cold cracking usually occurs when the alloy is in its brittle state, i.e. at a relatively low temperature [3]. This type of cracking can occur catastrophically and therefore, presents also a safety hazard.

In this work, we use process simulation software called ALSIM that is specially tuned for aluminum DC casting. ALSIM is able to predict defects that might arise during DC casting such as air gap formation, porosity and both types of cracking. The main goal of this work is to perform

benchmarking between DC casting simulation in ALSIM and trial DC casting. This is to validate the crack susceptibility model with respect to different casting parameters. We performed casting trials with different casting conditions such as: casting speed and cooling rate, also changing the inlet geometry. By varying these parameters, we expect to observe the effect of fluid flow on both types of cracking susceptibility. In addition, since we have performed a simultaneous prediction of both cracks, we also expect to observe the possible connection between the two types of cracking as explained by Lalpoor et al. [4] and we will try to formulate the possible mechanism of such connection based on ALSIM calculation.

The result of this work provide a better understanding for the interpretation of cracking prediction in ALSIM and also assist the modeling efforts on the connection between hot tearing and cold cracking.

2. DC casting modeling in ALSIM

ALSIM is a finite element package with the capability to perform a coupled calculation between thermal, fluid flow and mechanical phenomena. A more detailed description regarding the ALSIM software and its physical model (thermal, fluid-flow and mechanical models) can be found elsewhere [5, 6]. In order to predict the behavior of a certain alloy during DC casting, ALSIM needs several inputs, such as the solidification path of the alloy. In addition, ALSIM needs specific information regarding the thermal, fluid and mechanical properties of the alloy, which can be obtained either using model prediction software or through experiment [4]. In the next sub-section, we provide a brief description of how ALSIM performs the heat transfer and mechanical calculations during DC casting.

2.1. Heat transfer and mechanical calculation phenomena

Heat transfer is a vital phenomenon during DC casting because it defines the solidification front, convective fluid flow, and temperature gradients which in turn governs the sump geometry and mechanical response of the alloy during the casting process. In this simulation the primary heat extraction occurs through the mold and bottom block. We assume the heat transfer coefficient of both of the cooling surface is approximately 1000 W/m^2K. However, during DC casting, often air gap is formed at the lower part of the mold, due to the thermal contraction of the ingot which reduces the heat transfer between the ingot and the mold. In ALSIM, this phenomenon is also taken into account for heat transfer calculation.

During casting the alloys undergoes phase transformation from liquid to solid which produces different mechanical behavior of the alloy in various domains of the ingot. ALSIM uses different constitutive model to represent behavior of the alloy in specific temperature ranges. At a very high temperature, where the material is fully liquid or at a low solid fraction, no mechanical calculations are performed. This is because we assumed that most of the mechanical forces are accommodated via grain translation and rotation due to the abundance of the fluid phase. At a higher solid fraction or at high temperature – fully solid state, indeed mechanical calculations are performed and the constitutive models used for these calculations are described elsewhere [7]. At the lower temperature – fully solid state, the constitutive behavior of the material is described by the extended Ludwik equation as described in [8].

The result from calculations with this constitutive behavior leads to the variables that are needed for the crack prediction calculation in ALSIM, which will be discussed in more detail in the next part.

2.2. Cracking criteria

In ALSIM, the hot tearing susceptibility is measured by taking into account both the feeding difficulties and thermal deformation effect, as these two phenomena are well known to be the main driving force for hot tearing during DC casting [9]. The criterion used is called the integrated critical strain or ICS and the formulation is as follows:

$$\Delta\varepsilon\left(w_v, w_d\right) = \begin{cases} 0 & \text{for } p_l \geq p_c \\ \int_{t(p_l < p_c)}^{t\left(g_s = g_s^{nof}\right)} \left(w_v \cdot \mathrm{tr}\left(\dot{\varepsilon}_s^p\right) + w_d \cdot \bar{\dot{\varepsilon}}_s^p\right) dt & \text{for } p_l < p_c \end{cases} \quad (1)$$

ICS ($\Delta\varepsilon$) measures the amount of deformation (through the plastic strain rate or $\dot{\varepsilon}_s^p$) that occurs when the mush is vulnerable to hot tearing, namely when it is in a state of feeding difficulties and the pressure in the mushy zone (p_l) is below a certain critical pressure (p_c). This calculation is finished when the solid fraction of the mush (g_s) has passed through the advanced coalescence stage ($g_s > g_s^{nof}$), because at this solid fraction, we assume that coalescence and bridging between the grains are fairly advanced, therefore no continuous liquid films are present. Thus, the alloy has obtained sufficient ductility to prevent the formation of a hot tear. The parameters w_v and w_d enable us to tune the weight of the calculation between volumetric and deviatoric strain components respectively. More details of this criterion could be found elsewhere [7].

For cold cracking, ALSIM measures the cracking susceptibility via the critical crack size or CCS. The principle idea of such criterion is as follows; if a defect (for instance: micro hot-tear, inclusion or porosity) exists within the ingot and such a defect has a dimension exceeding the CCS at a temperature of brittle fracture, then cold cracking will occur. The formulations of cold cracking criteria for different crack geometries [3] are shown in Table 1.

Table 1. Geometrical factor of different types of cracks [3]. a_c is half of CCS, K_{Ic} is plane strain fracture toughness and σ_{11} is the first principal stress.

Penny-shaped crack	Thumbnail-shaped crack
$a_c = \frac{\pi}{4}\left(\frac{K_{Ic}}{\sigma_{11}}\right)^2$	$a_c = \frac{\pi}{(2\times 1.13)^2}\left(\frac{K_{Ic}}{\sigma_{11}}\right)^2$

The half of CCS (a_c) takes into account the geometry of the initial defect; whether it is a volumetric crack (penny-shaped crack) or a surface crack (thumbnail shaped crack). This criterion also takes into account the plane strain fracture toughness (K_{Ic}) from several temperature points, which are obtained experimentally [4] and the first principal stress σ_{11}, which is readily available from ALSIM calculations.

2.3. Simulation setup

In this work, we performed benchmarking between 2D DC casting simulations with trial DC casting billets. Owing to the geometric symmetry, to reduce the calculation time, we only performed the simulation on half of the geometry with the centerline of the ingot as the symmetry axis.

The simulated geometries are built according to the trial setup, which includes the melt distributor, mold, water jet, bottom block and ingot part or cast domains, i.e. the Euler, expansion and Lagrange domains (see Figure 1a). These geometries are meshed using quadrilateral elements. When the casting starts and the first part of the billet has been solidified, the bottom block will be retracted downwards and elements in the expansion zone will grow every time step vertically until a new row of elements is splitted from the expansion zone and added to the Lagrange domain below. Subsequently, the ingot shell which has just solidified is sprayed with water at room temperature and after the casting is finished, the ingot is continuously sprayed with room temperature water for several minutes to cool down.

Other than varying the casting speed and water flow rate, we also use two different inlet geometries; a semi-horizontal feeding scheme (Figure 1b) which has two flow directions – downward vertical and horizontal to the periphery of the billet and a vertical feeding scheme (Figure 1c) which has only downward vertical flow direction.

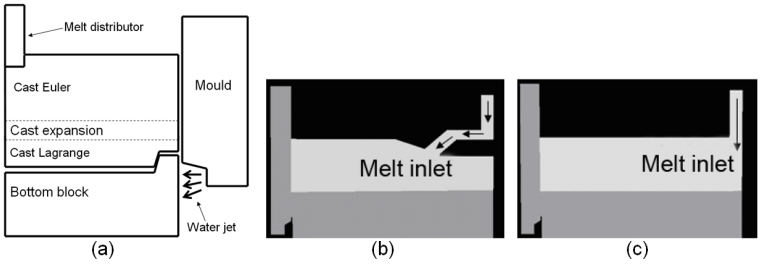

Figure 1. Generic casting setup geometry (a) and two different types of inlet flow geometry; semi-horizontal feeding scheme (b) and vertical feeding scheme (c).

The solidification path of an AA7050 alloys was calculated using JMat-Pro software. For the constitutive mechanical behavior prediction, an Al–2 wt% Cu database was used for the mushy zone regime [10], since the AA7050 data in this temperature regime is not available. For the fully solid temperature regime we used the database of an AA7050 alloy [4].

For calculation of hot tearing susceptibility, we used a critical pressure of –7000 Pa and a g_s^{nof} of 0.99. The weights for volumetric and deviatoric strain components were 1.0 and 0.0, respectively. For the cold cracking susceptibility calculation, we used our own data for plane strain fracture toughness (K_{Ic}) of the AA7050 alloy and we assumed that the initial crack geometry is penny shaped.

We performed three different casting trials with different casting conditions and the result of those castings were billets with hot tears, cold cracks and a healthy ingot without visible fracture. The details of the trial casting information are described in the next section.

3. Procedure of casting trials

The cylindrical billets were DC cast at Tata Steel Research and Development centre in IJmuiden, The Netherlands. The diameter of the ingot was 315 mm and the nominal composition of the ingots is shown in Table 2. The melt was first degassed in the furnace at 730 °C and then cast with a conventional DC casting mold as shown in Figure 1a. The casting temperature was approximately 680 °C. All of the billets were grain refined by using the same amount of Al5Ti1B for each ingot.

Table 2. Chemical composition of AA7050.

Main Alloying Elements, wt pct					
Zn	Cu	Mg	Zr	Ti	Al
6.15	2.2	2.1	0.13	0.03	balance

Table 3. Description of the casting process parameters for the AA7050 alloy.

Process parameter	Ingot 1	Ingot 2	Ingot 3
Distributor/inlet geometry	Vertical	Semi-horizontal	Semi-horizontal
Nominal casting speed (mm/min)	50	90	50
Water flow rate (l/min)	40	110	40
Cracking status	Hot tear	Cold crack	Healthy

We performed three DC casting trials with different casting parameters shown in Table 3. As a result, we have one billet with hot tear, one with cold crack and one healthy ingot that we will use as a reference. The nominal casting speed and water flow rate correspond to the steady state casting conditions after the ramping up stage.

4. Result and discussion

Figure 2 shows the cracked billets. The hot tear is shown in Figure 2a. One can see a centerline crack (between the arrow heads) that propagates as a plane along the longest axis of the ingot. This is the classical feature of a catastrophic hot tear [11], because such a crack is produced through tensile-radial

mechanical deformation of the semi-solid mush due to the high temperature gradient between the center and the surface of the billet.

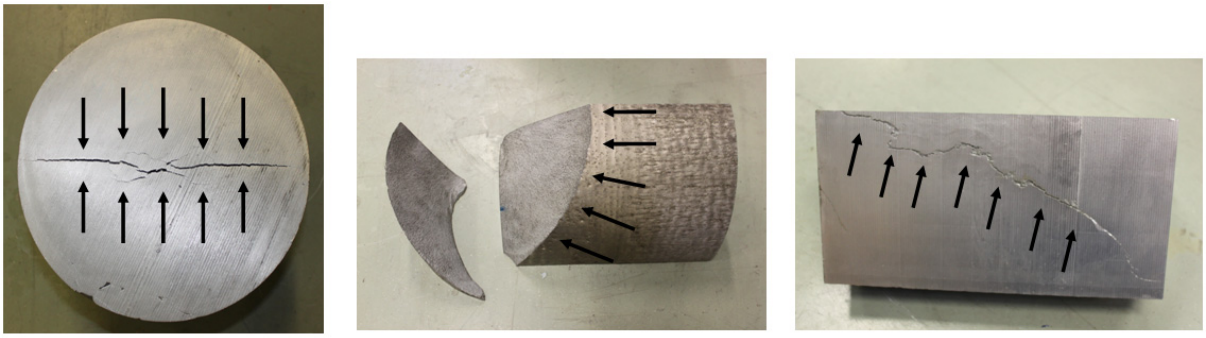

Figure 2. Ingot with hot tear (a) and ingot with cold crack which occurs throughout the ingot (b, c).

Figures 2b and 2c show cold cracked part of the other billet. These figures demonstrate that the cracks are propagating throughout the billet but not necessarily propagate through the centerline. For instance, in Figure 2b, the crack that splits the billet open starts from the centerline and propagates to the surface (pointed by the arrows). In Figure 2c, one can see a crack path (pointed by the arrows) of a cold crack that has not split the billet apart.

4.1. Simulation results

In Figure 3, we can see examples of ALSIM calculation from the healthy billet case. These results are taken at a simulation time of 650 seconds or when the ingot reaches a length of 500 mm (in the steady state casting condition).

Figure 3a shows a parabolic-shaped contour which roughly represents the sump shape of the ingot. In Figure 3b, one can see that areas with high tensile stresses are located in the center of the ingot and nearby the water impingement zone, and the surface part is under low tensile stress or compressive stress. Figure 3c demonstrates that the pressure is decreasing with increasing solid fraction, and reaches the lowest value in the bottom of the sump and near the mold. This phenomenon signifies the feeding difficulty which is well captured by the model. Figures 3d and 3e represents hot tearing susceptibility through ICS and cold cracking susceptibility through CCS respectively. For ICS, we can see that the highest amount is on the centerline of the ingot and the value peaked just above the bottom block, representing the startup stage of the casting. This result supports the previous findings [7, 12]. Meanwhile for cold cracking susceptibility, we can see that the center of the ingot is more prone to cold cracking than the surface, which also supports another previous work [13]. The area which has a negative CCS value (area pointed to by the arrows) has temperatures higher than 200 °C, thus no calculation is performed in this temperature regime since the state of the material at such temperatures is not favorable for cold cracking.

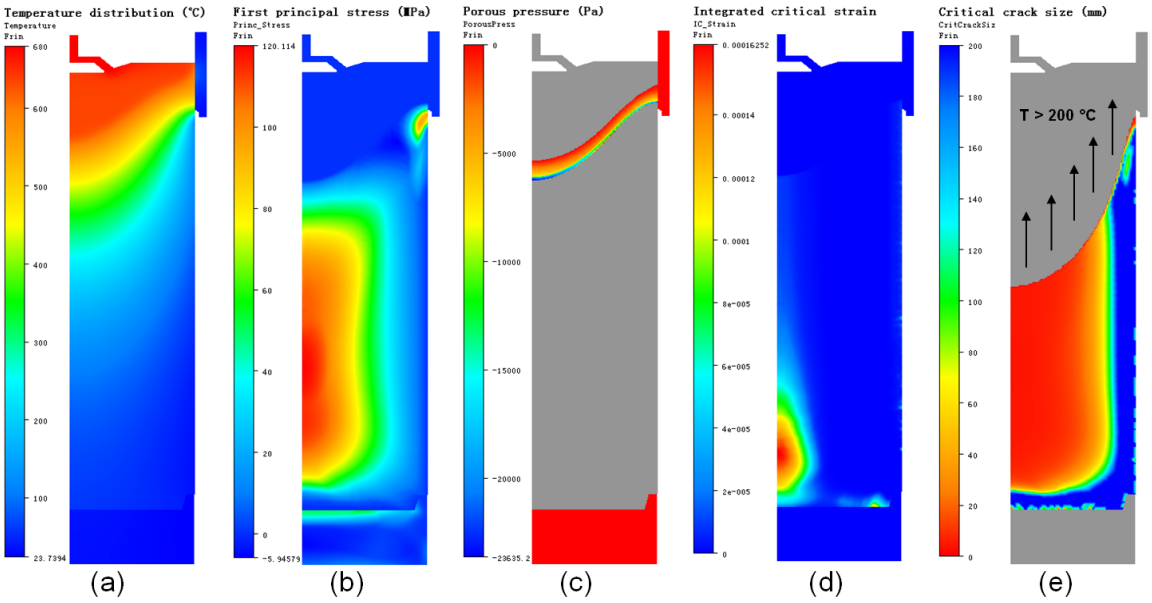

Figure 3. Example of calculation results for the healthy billet at the steady-state casting condition: temperature distribution in °C (a), first principal stress in MPa (b), porous pressure in Pa (c), integrated critical strain in arbitrary unit (d) and critical crack size in milimeter (e).

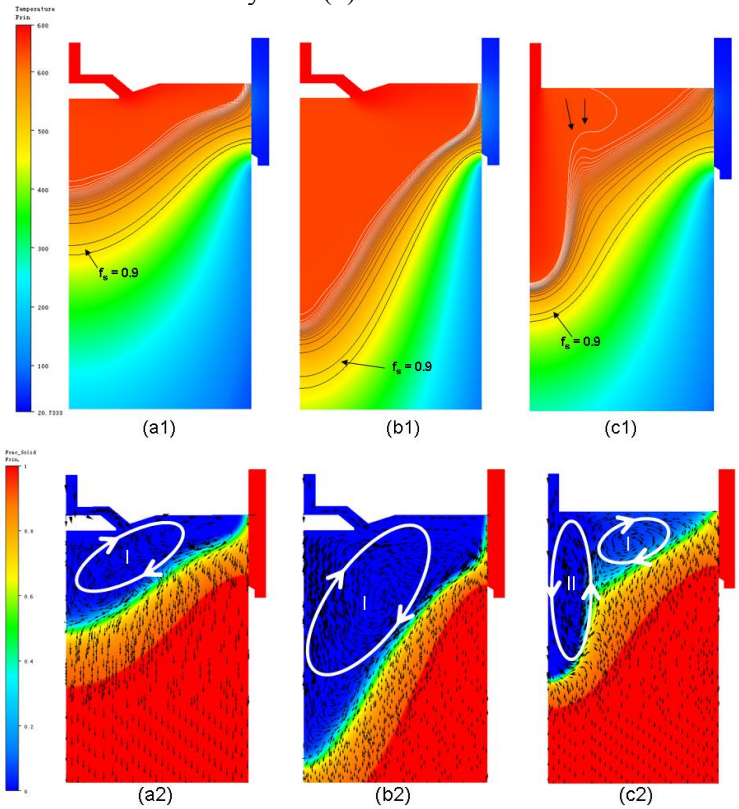

Figure 4. Comparison of temperature distribution in °C and solid fraction isolines – between 0 and 1 (a1, b1 and c1) and comparison of solid fraction and fluid flow, in the sump (a2, b2 and c2) for different cases. a – healthy, b – cold crack and c – hot tear.

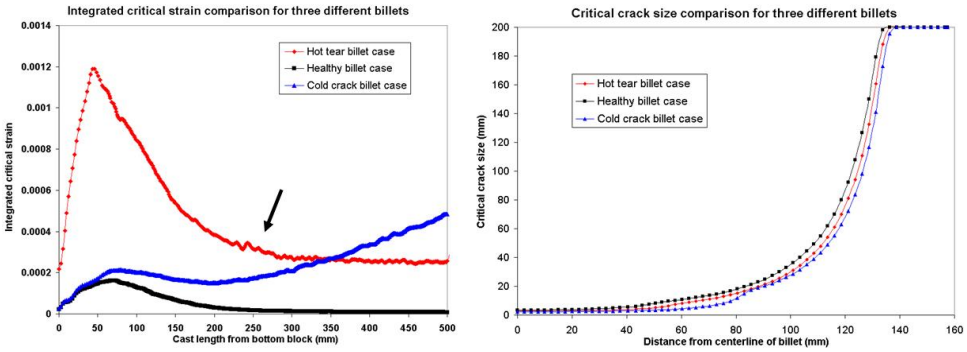

Figure 5. Examples of ICS comparison (a) and CCS comparison (b) for the three different cases.

In Figure 4 (a1, b1, c1), we can see the different sump shapes and depths for the different cases. All of these results are in the steady-state casting stage. In terms of sump depth (from metal level down to a solid fraction (f_s) of 0.9), the deepest sump occurs in the cold cracking case with a depth of 253 mm while the hot tear case has a depth of 176.5 mm and the shallowest sump corresponds to the healthy ingot with a depth of 140 mm. Although the depth varies significantly between the healthy and the cold-crack cases, the sump shape is similar and the sump depth increases linearly with casting speed. The sump geometry changes significantly when the inlet flow is changed. This is apparent when we compare the healthy and the hot tearing cases. Although the casting speed is the same, the difference in terms of sump geometry and depth is remarkable. This difference is believed to be due to the flow pattern produced by the different inlet geometries.

We also observed the flow patterns of each case at the steady-state casting condition. In the healthy case, there is only one dominating flow (pattern I within white ellipse – Figure 4 a2). This condition is also holds true for the cold-crack case (pattern I within white ellipse – Figure 4 b2). The dominating flow in both case are in the same direction, along with the natural convective flow. In the hot tearing case, however there are two dominating flows with different flow directions (pattern I is clockwise and pattern II is counter-clockwise – Figure 4 c2). These flows intersect in a region of approximately 49 mm from the ingot centerline, thus in this area there is almost no horizontal velocity component. The model also responds quite well to this phenomenon where there is a discontinuous sump gradient in this particular region (the steeper sump beside pattern II and the shallower sump beside pattern I). The variation in the flow results in a very variable sump profile especially at a lower solid fraction (denoted by the arrow heads in Figure 4 c1).

Figure 5a shows the hot tear susceptibility along the centerline of the billet from the bottom block up to 500 mm of billet height. For all of the cases, the ICS values reaches a high peak in the start-up stage, which is a common phenomenon during DC casting [7], and either vanish (healthy billet) or stabilize to a certain value (hot-tear and cold-crack cases) when entering the steady state. In the cold-crack case, after the decrease in the post startup phase, the ICS value increases but finally stabilizes at approximately 0.0006 after about 700 mm of billet length. We believe that the evolution of ICS value in such a case is due to the increase of casting speed which is almost twice of the healthy case. Although the sump in the cold crack case is the deepest among all given cases, the ICS at the startup is similar to the healthy case. The peak ICS value in the startup stage for hot tear case is approximately six times higher than for the other cases and the catastrophic hot tear was observed when the billet length reaches 250 mm (pointed by the arrow).

For cold cracking susceptibility calculation, we plotted in Figure 5b, the susceptibility at 500 mm of billet height, from the center to the surface. In general, the CCS increases dramatically after reaching the mid-radius of the ingot. We can also see that generally the cold-crack case has the lowest CCS value compared to other cases which means the highest susceptibility to cold crack is in accordance with the experimental trials.

Based on the hot tear susceptibility calculation, in the cold-crack case, after the billet reaches 700 mm of cast length, the ICS value stabilizes to a value which is approximately three times of the peak value during the start up stage. This result can be interpreted as the possibility of formation of micro (non-critical) hot tears that, due to the stress condition in the billet at high temperature and the ingot ductility [4], will not develop until the casting is finished and the billet has cooled down to its brittle state. This result supports the hypotheses about the connection between hot tearing and cold cracking [4].

5. Conclusion

From the result of this work, we draw several conclusions as follows:

1. The melt feeding scheme affects the shape of the sump by distributing hot melt and changing the temperature profile which plays an important role in the susceptibility to hot tearing in the billet.
2. Sump depth also increases with casting speed which in turn increases the thermal gradient between the centre and the surface of the billet and ultimately promotes hot tearing and cold cracking.
3. From ALSIM calculations, we obtained a supporting argument for the connection between the two cracks; cold cracks could be initiated from non-critical micro hot tears.
4. The output of the simulation is in qualitative agreement with the experimental results of trial DC casting which validates the cracking model used in ALSIM.

Acknowledgements

This research was carried out within the Materials innovation institute (www.m2i.nl) research framework, project number M42.5.09340. The authors would like to express their gratitude to Dr. Démian Ruvalcaba and Mr. Jacob van Oord (Tata Steel Research, Development & Technology, The Netherlands) for their support and inputs. Support from Modelling assisted INnovation for Aluminum DC Casting process (MINAC) community is highly appreciated.

References

[1] Granger D A 1989 *Aluminum Alloys–Contemporary Research and Applications* (London: Academic Press) pp 109-135
[2] Lalpoor M, Eskin D G and Katgerman L 2008 *Materials Science and Engineering A* **497** 186
[3] Lalpoor M, Eskin D G and Katgerman L 2010 *Metallurgical and Materials Transactions A* **Vol. 41A** 2425
[4] Lalpoor M, Eskin D G and Katgerman L 2009 *Metallurgical and Materials Transactions A* **Vol. 40A** 3304
[5] Mortensen D, Fjær H G, Lindholm D, Rudshaug M and Sørheim E A 2011 *Materials Science Forum* **693** 187
[6] Mortensen D 1999 *Metallurgical and Materials Transactions B* **Vol. 30B** 119
[7] M'Hamdi M, Mo A and Fjær H G 2006 *Metallurgical and Materials Transactions A* **Vol. 37A** 3069
[8] Fjær H G and Mo A 1990 *Metallurgical Transactions B* **Vol. 21B** 1049
[9] Eskin D G, Suyitno and Katgerman L 2004 *Progress in Materials Science* **49** 629
[10] Ludwig O, Drezet J-M, Martin C L and Suery M 2005 *Metallurgical and Materials Transactions A* **Vol. 36A** 1525
[11] Suyitno, Eskin D G, Savran V I and Katgerman L 2004 *Metallurgical and Materials Transactions A* **Vol. 35A** 3551
[12] Drezet J -M, M'Hamdi M, Benum S, Mortensen D and Fjaer H 2002 *Materials Science Forum*, **396** 59
[13] Lalpoor M, Eskin D G, Ruvalcaba D, Fjær H G, Ten Cate A, Ontijt N and Katgerman L 2011 *Materials Science and Engineering A* **528** 2831